J. Mater. Environ. Sci. 4 (1) (2013) 127-138
ISSN : 2028-2508
CODEN: JMESCN

Green corrosion inhibitor: inhibitive action of tannin extract of *Chamaerops humilis* plant for the corrosion of mild steel in 0.5 M H_2SO_4

O. Benali [1,]*, H. Benmehdi [2], O. Hasnaoui [1], C. Selles [3], R. Salghi[4]
[1]*Department of Biology, Faculty of Sciences and Technology ,Univesrity Dr Moulay Tahar - Saïda (Algeria)*
[2] *Department of Engineering Procedures, University of Bechar 08000 Algeria.*
[3]*Laboratory of LASNABIO, Department of Chemistry, University of Tlemcen 13000 Algeria.*
[4]*Equipe de Génie de l'Environnement et de Biotechnologie, ENSA, Université Ibn Zohr, BP 1136 Agadir, Morocco*

Received 08 Aug 2012, Revised 11 Sept 2012, Accepted 11 Sept 2012
*Corresponding author. Email: benaliomar@hotmail.com

Abstract

The corrosion and inhibition behaviors of mild steel in sulfuric acid + 5% EtOH in the presence of tannin extract of *Chamaerops humilis* plant **(LF-Ch)** and potassium iodide (KI) have been studied using the electrochemical methods. It was found that the inhibition efficiency increased with **LF-Ch** extract concentration. The addition of potassium iodide to **LF-Ch** extract in solution increased the inhibition efficiency of this latter. A synergistic effect was observed between KI and extract with optimum of concentration of 100 mg /L **LF-Ch** extract + 0.025% potassium iodide. Adsorption of extract alone or in combination with potassium iodide on the metal surface obeyed the Langmuir adsorption isotherm and thermodynamic calculations revealed that the adsorption of inhibitor were of chemical nature. That suggest the presence of iodide ions in solution increases the surface coverage. The adsorption of **LF-Ch** extract on the mild steel in aggressive medium leads to the formation of a protective film which grows in thickness and effectiveness with increasing exposure time.

Keywords: Mild steel, corrosion test, electromechanical techniques, adsorption, synergistic effect.

1. Introduction

Corrosion problems in the oil and petrochemical industry usually have been solved by the selection of suitable materials and/or by changing the environment to make it less aggressive [1]. Acid solutions are widely used in the industry. The most important areas of application are acid pickling, industrial acid cleaning, acid descaling and oil well acidizing [2]. Corrosion inhibitors are needed to reduce the corrosion rates of metallic materials in these acid media [3-8]. An inhibitor is usually added in small amount in order to slow down the rate of corrosion through the mechanism of adsorption [9-10]. Over the years, several inhibitors have been synthesised or chosen from existing compounds and it has been found that the best inhibitors are those that have centre for π electron donation (usually enhanced by the presence of hetero atoms in aromatic compound) while others may be gotten from extracts of naturally occurring compounds [11-13]. The last class of inhibitors (green inhibitors) are significant because they are non toxic and do not contain heavy metals hence they are environmentally friendly [14-15]. The present study is aimed at investigating the inhibitive and adsorption properties of tannin extract of *Chamaerops humilis (LF-Ch)* for the corrosion of mild steel in H_2SO_4.

2. Experimental

2. 1. Plant Material

The leaves and fruits pericarp of the *Chamaerops humilis* **(LF-*Ch*)** plant were collected from mountains located at western Algeria (Tlemcen area) in july 2011. From a geographical point of view, the districts are located, respectively in the mountains of Trara (3 districts: Djebala, Fillaoucene, Ronaine) and in the mounts of Tlemcen (2 districts: Oued Chouly (currently Oued Lakhdar) and Azails). The plant sample was identified by the authors. The voucher specimen was deposited in the Biological Science laboratory of the ecology, Department of Biology - University Abou Bakr Belkaid of Tlemcen.

The plant organs were cut into small pieces and shade dried at room temperature (20°C) for two weeks, finely powdered plant materials were stored in airtight polythene bags protected from sunlight until use.

2. 2. Preparation of the tannins extract

A total of 425 g of defatted powder of each parts (leaves or pericarp fruit) were contacted with 1700 mL of acetone/water (70:30, v/v) in 2000 mL capped flask with timely shaking and stirring for 4 days at ambient temperature (maceration). The obtained extract was filtered by using Whatmann filter paper and then acetone was removed from the extract by using a rotary evaporator. The aqueous extract was extracted respectively with dichloromethane (2x100 mL) and 4x100 mL with diethyl acetate. The organic layer (AcOEt) was dried with Na_2SO_4, filtered and concentrated to dryness to give crude extract of tannins as a brownish solid (m=1,9g; yield=0,446%; mp=110-120°C) [16]. The Phytochemical investigation of leaves and fruits extracts of this plant was done in detail in our previous work [17].

2. 3. Solution and material

A 0.5 M H_2SO_4 solution was prepared from an analytical reagent grade of H_2SO_4 98% and distilled water + 5% of Ethanol absolute and was used as corrosion media in the studies.

For the electrochemical measurements, the experiments were carried out in solution of 0.5 M sulfuric acid +5 % Ethanol (uninhibited and inhibited) on mild steel of composition (wt%) : $C \leq 0.1\%$, $Si \leq 0.03\%$, $Mn \leq 0.2\%$, $P \leq 0.02\%$, $Cr \leq 0.05\%$, $Ni \leq 0.05\%$, $Al \leq 0.03\%$ and the remainder iron. Specimens in the form of disc were abraded successively with different grades of emery paper up 1200 grade.

2. 4. Electrochemical measurements

Electrochemical experiments were carried out in a glass cell (CEC/TH-Radiometer) with a capacity of 500 mL. A platinum electrode ($1 cm^2$) and a saturated calomel electrode (SCE) were used as a counter electrode and a reference electrode, respectively. The working electrode (WE) was in the form of a disc cut from mild steel under investigation and was embedded in a Teflon rod with an exposed area of $0.5 cm^2$.

Electrochemical impedance spectroscopy (EIS), potentiodynamic and linear polarization were conducted in an electrochemical measurement system (VoltaLab40) which comprises a PGZ301 potentiostat, a personal computer and VoltaMaster 4 and Zview software. The potentiodynamic current–potential curves were recorded by changing the electrode potential automatically from –800 to –200 mV with scanning rate of 2 mV s^{-1}. The polarization resistance measurements were performed by applying a controlled potential scan over a small range typically 10 mV with respect to E_{corr}. The resulting current is linearly plotted against potential, the slope of this plot at E_{corr} being the polarization resistance (Rp). All experiments were carried out in freshly prepared solution at constant temperature 32 ± 0.1 °C using a thermostat. The ac impedance measurements were performed at corrosion potentials (E_{corr}) over a frequency range of 10 kHz – 100 mHz, with a signal amplitude perturbation of 10 mV. Nyquist plots were obtained.

From the measured polarization resistance value, the inhibition efficiency has been calculated using the relationship:

$$IE_{Rp}\,(\%) = \ 1 - \frac{R_{0p}}{R_{ip}} \times 100 \tag{1}$$

where R_{0p} and R_{ip} are the polarization resistance in absence and in presence of inhibitor, respectively. The inhibition efficiency was evaluated from the measured I_{corr} values using the relationship:

$$IE_{Icorr}\,(\%) = \ 1 - \frac{i_{icorr}}{i_{0corr}} \times 100 \tag{2}$$

where i_{0corr} and i_{icorr} are the corrosion current density in absence and in presence of inhibitor, respectively.

The inhibition efficiency was evaluated from the calculated Corrosion rate (C.R) using the relationship:

$$IE_{C.R}\,(\%) = \ 1 - \frac{C.R}{C.R_0} \times 100 \tag{3}$$

where $C.R_0$ and C.R are the corrosion rate in absence and in presence of inhibitor, respectively.

The inhibition efficiency of the inhibitor has been found out from the charge transfer resistance values using the following equation:

$$IE_{Rt}\,(\%) = \ 1 - \frac{R_{0t}}{R_{it}} \times 100 \tag{4}$$

where R_{0t} and R_{it} are the charge transfer resistance in absence and in presence of inhibitor, respectively.

3. Results and discussion

3. 1. Polarization measurements

Potentiodynamic anodic and cathodic polarization scans were carried out at 32±0.1 °C in 0.5 M H_2SO_4 +5% EtOH with different concentrations of **LF-*Ch*** extract. Anodic and cathodic polarization curves in the absence and in the presence of inhibitor at different concentrations after 30 min of immersion are shown in Figure 1. From this figure, it can be seen that with the increase of **LF-*Ch*** extract concentrations, both anodic and cathodic currents were inhibited. This result shows that the addition of **LF-*Ch*** extract inhibitor reduces anodic dissolution and also retards the hydrogen evolution reaction.

Table 1 gives the values of kinetic corrosion parameters as the corrosion potential E_{corr}, corrosion current density I_{corr}, Tafel slopes (b_c and b_a) and inhibition efficiency for the corrosion of mild steel with different concentrations of **LF-*Ch*** extract. The corrosion current densities were estimated by Tafel extrapolation of the cathodic and anodic curves to the open circuit corrosion potential.

From this table, it can be concluded that:

- The I_{corr} values decrease with increasing inhibitor concentration.
- The cathodic Tafel slopes were found to vary over a range of 314 - 222 mV dec^{-1}. Therefore, the cathodic slope value was found to change with increasing concentration of **LF-*Ch*** extract in aggressive solutions. This result indicates the influence of the inhibitor on the kinetics of the hydrogen evolution reaction [8].
- The anodic Tafel slopes were found to vary over a range of 231 - 126 mV dec^{-1}. Therefore, the anodic slope value was found to change with increasing concentration of **LF-*Ch*** extract in aggressive solutions. This result indicates the influence of the inhibitor on the kinetics of the dissolution of the mild steel.
- The values of inhibition efficiency (P %) increase with inhibitor concentration reaching a maximum value (78.55%) at 100 mg /L.

- The **LF-*Ch*** extract is a mixed inhibitor.

On the other hand, the Corrosion Rate was determined by the conversion of the corrosion current density (I_{corr}) by using the expression [18-19]:

$$C.R\,(\frac{mm}{Year}) = 3.268x10^{-3}\,(\frac{i_{corr}}{n.\rho}.M_{Fe}) \qquad (5)$$

Where M_{Fe} is the molecular weight of steel, n is the number of electrons transferred in the corrosion reaction, and ρ is the density of Fe (g . cm^{-3}).

Table 2 gives the values of the corrosion rate (C.R), the polarisation resistance (R_p) and inhibition efficiency for the corrosion of mild steel with different concentrations of **LF-*Ch*** extract.

From this table, it can be concluded that:

- The C. R values decrease with increasing inhibitor concentration and the Rp values vary in the opposite direction.
- The values of inhibition efficiency (P %) increase with inhibitor concentration reaching a maximum value (78.50%) at 100 mg /L.

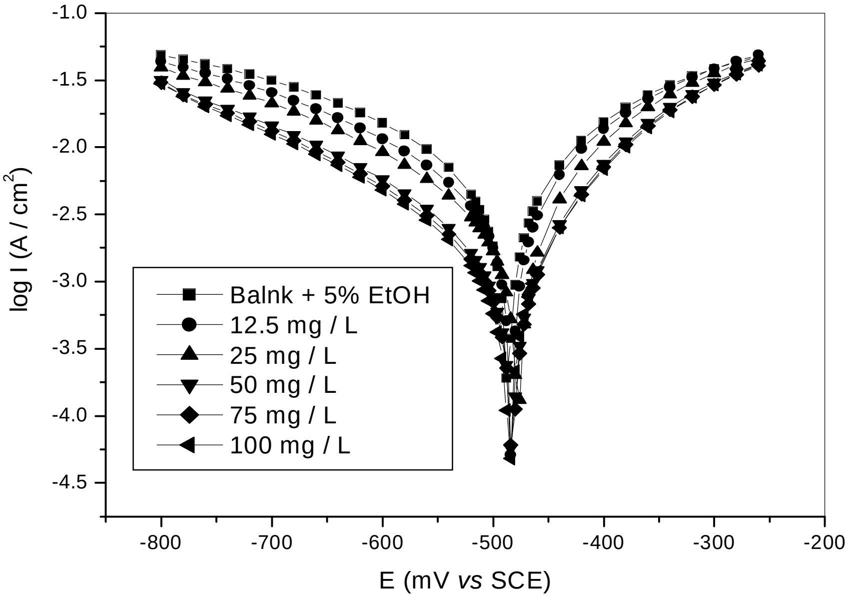

Figure 1. Potentiodynamic polarization curves for mild steel in 0.5 M H_2SO_4 +5% EtOH containing different concentrations of **LF-*Ch*** extract at 32 °C.

Table 1. Electrochemical parameters and the corresponding corrosion inhibition efficiencies for the corrosion of mild steel in the presence of different concentrations of **LF-*Ch*** extract at 32 °C.

Conc. (mg/L)	**E_{corr} (mV vs CSE)**	**I_{corr} (mA /cm^2)**	**b_a (mV/dec)**	**$-b_c$ (mV/dec)**	**P% (I_{corr})**
Blank	-487	6.9	231	314	----
12.5	-484	4.21	164	265	**38.98**
25	-478	2.99	138	249	**56.67**
50	-483	1.85	133	234	**73.18**
75	-483	1.59	126	228	**76.96**
100	-486	1.48	127	222	**78.55**

Table 2. Electrochemical parameters and the corresponding corrosion inhibition efficiencies for the corrosion of mild steel in the presence of different concentrations of **LF-*Ch*** extract at 32 °C.

Conc. (mg/L)	**Rp (Ω.cm^2)**	**C.R (mm/Y)**	**P% (R_P)**	**P% (C.R)**
Blank	6.85	80.72	**----**	**-----**
12.5	10.75	49.28	**36.28**	**38.95**
25	13.85	34.98	**50.54**	**56.66**
50	22.50	21.69	**66.40**	**73.13**
75	25.30	18.58	**72.92**	**76.98**
100	27.65	17.35	**75.23**	**78.50**

3. 2. Electrochemical impedance spectroscopy measurements

- Nyquist plots of mild steel in 0.5 M H_2SO_4 + 5% EtOH in the presence and absence of different concentrations of **LF-*Ch*** extract at 32°C and after 0.5 h of immersion are given in Figure 2. All the plots display a single capacitive loop [20]. Impedance parameters derived from the Nyquist plots and percent inhibition efficiencies are given in Table 3.

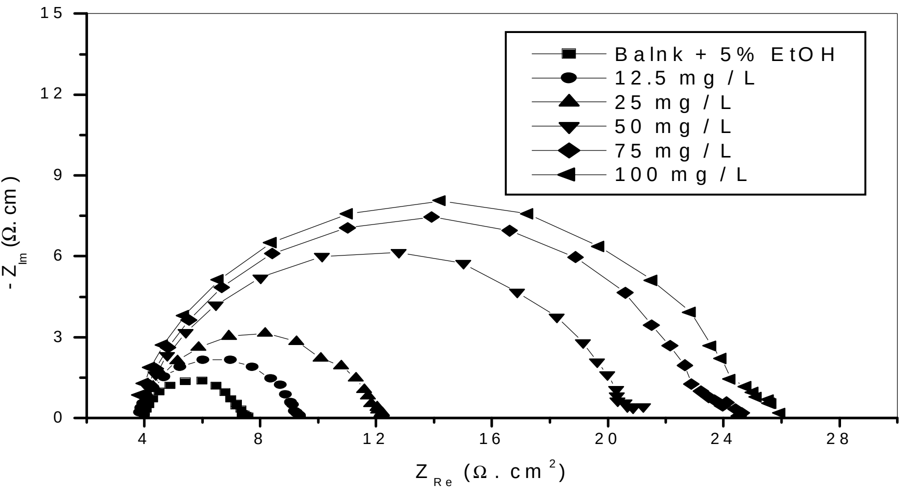

Figure 2. Complex plane plots for mild steel in the aggressive solution in the absence and in the presence of different concentrations of **LF-*Ch*** extract at 32°C.

The circuit consists of a constant phase element (CPE) Q, in parallel with a resistor R_t The use of CPE-type impedance has been extensively described [21–23]:

$$Z_{CPE} = [Q(jw)^n]^{-1} \tag{6}$$

The above equation provides information about the degree of non-ideality in capacitance behavior. Its value makes it possible to differentiate between the behavior of an ideal capacitor (n = 1) and of a CPE (n < 1).

Considering that a CPE may be considered as a parallel combination of a pure capacitor and a resistor that is inversely proportional to the angular frequency,

the value of capacitance, C_{dl}, can thus be calculated for a parallel circuit composed of a CPE (Q) and a resistor (R_t), according to the following formula [24, 25]:

$$Q = \frac{(c_{dl} R_t)^n}{R_t} \tag{7}$$

The impedance spectra of mild steel in 0.5 M H_2SO_4 with and without inhibitor were analyzed by using the circuit in Figure 3, and the double layer capacitance (C_{dl}) was calculated in terms of Eq. 7. Values of elements of the circuit corresponding to different corrosion systems, including values of C_{dl}, are listed in Table 3.

As can be seen from Table 3, the increase in resistance in the presence of **LF-*Ch*** extract compared to H_2SO_4 alone is related to the corrosion protection effect of the phytochemical constituents. The value of C_{dl} decreases in the presence of **LF-*Ch*** extract, suggesting that the extract plant molecules function by adsorption at the metal solution/interface. It is important to point out that n decreases with the increase of the concentration and reaches a value of 0.80. This shows an increase of the surface inhomogeneity as a result of the inhibitor's adsorption [5]. The values of inhibition efficiency increase with inhibitor concentration at a maximum value (**84.52%**) at 100 mg /L.

Table 3 . Impedance parameters and inhibition efficiency for the corrosion of mild steel in 0.5 M H_2SO_4 + 5% EtOH containing different concentrations of **LF-*Ch*** extract at 32°C

Conc. (mg/ L)	**Q ($s^n\Omega^{-1}.cm^{-2}$)**	**n**	**R_t ($\Omega.cm^2$)**	**C_{dl} (μ F cm^{-2})**	**P (%)**
Blank	$4.9x10^{-4}$	0.84	3.56	146.15	-----
12.5	$2.8x10^{-4}$	0.85	5.55	87.94	**35.85**
25	$3.03x10^{-4}$	0.80	8.45	68.16	**57.87**
50	$1.40x10^{-4}$	0.81	17.11	34.0	**79.19**
75	$1.25x10^{-4}$	0.81	20.23	30.74	**82.40**
100	$1.15x10^{-4}$	0.80	23.00	26.36	**84.52**

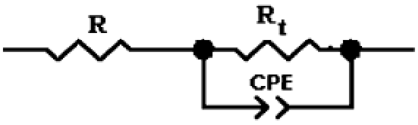

Figure 3. The equivalent circuit of the impedance spectra obtained for **LF-*Ch*** extract.

On the other hand, the excellent behaviour of LF-*Ch* extract previously indicated in the potentiodynamic polarization measurements is confirmed. Figure 4 gives the inhibition efficiency of LF-*Ch* extract in aggressive medium calculated by different methods.

3. 3. Synergistic consideration

Halides ions have been widely reported to synergistically increase the inhibition of the corrosion of metals in acidic medium by organic compounds [26-31]. The enhanced corrosion inhibition on addition of the halides was attributed to promotion of the adsorption of the organic molecules on the metal surface. The effect of KI on the inhibition efficiency of **LF-*Ch*** extract was investigated in the present work at 32°C. Figure 5 shows the plot of different values of I_{corr} for the different concentrations of **LF-*Ch*** extract in the absence and presence of 0.025% KI at 32°C after 30 min of immersion. Similarly, Figure 6 shows the plot of I_{corr} values vs. KI concentration added to a fixed extracts' concentration (100 mg/L) for **LF-*Ch*** extract at 32°C after 30 min of immersion.

Figs. 5 and 6 clearly reveals the existence of synergism phenomenon between iodide ions and the **LF-*Ch*** extract considering that I_{corr} was decreased on addition of the iodide ions to the extracts in comparison to the extract alone. Table 4 gives the values of I_{corr} and inhibition efficiency for corrosion of mild steel in 0.5M H_2SO_4 + 5% EtOH with various concentrations of **LF-*Ch*** extract in the presence an absence of 0.025 per cent KI at 32 °C.

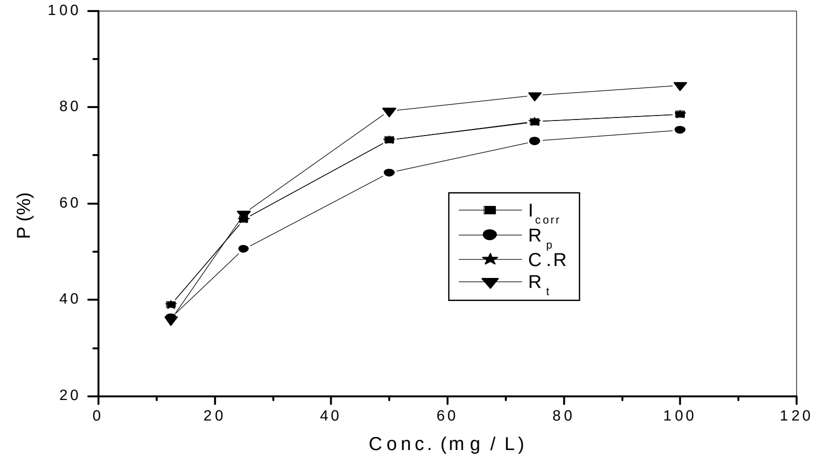

Figure 4. Inhibition efficiency *vs* inhibitor concentrations calculated by different methods

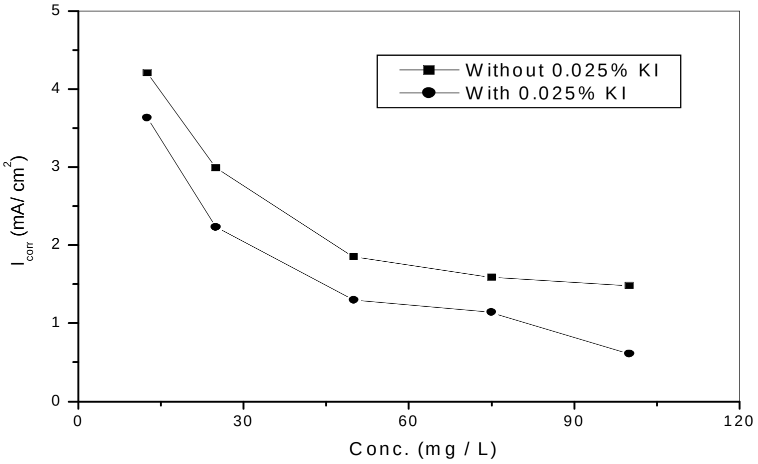

Figure 5. I_{corr} values in the absence and presence of 0.025% KI for different concentrations of **LF-*Ch*** extract.

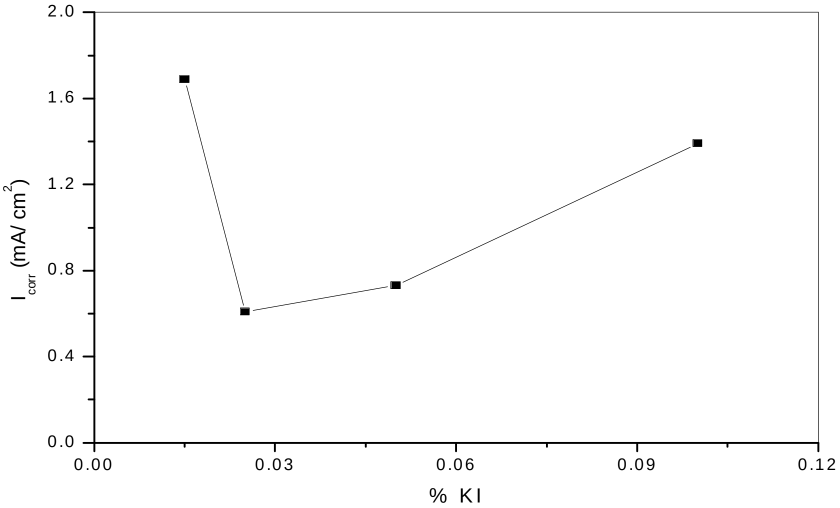

Figure 6. The plot of I_{corr} values vs. % KI for **LF-*Ch*** extract at 100 mg/L.

To evaluate the synergistic effects between the two inhibitors, synergism parameter (S) can be established as fallows [1]:

$$S = \frac{I_1 I_2}{I_{1,2} I_0} \tag{8}$$

Where I_o is corrosion current density for the blank solution; I_1 and I_2 are corrosion current densities in the presence of **LF-*Ch*** extract and KI, respectively; and $I_{1,2}$ corrosion current density in the presence of **LF-*Ch*** extract and KI, simultaneously. S approaches 1 when no interaction between the two inhibitors exists, while S>1 points to a synergistic effect. In the case of S<1, the antagonistic interaction predominates [32]. The corrosion current density in the presence of 0.01% KI was obtained from polarization curves. Table 5 gives values of the synergism parameter (S) which is calculated for different concentrations of **LF-*Ch*** extract and 0.025% KI, by using polarization curves data.

Table 4. I_{corr} values and Inhibition efficiency for corrosion of mild steel with different concentrations of **LF-*Ch*** extract in the presence of 0.025% KI at 32 °C.

Conc. (mg/L)	**I_{corr} (mA /cm^2)**	**P% (I_{corr})**
Blank	6.90	----
Blank +KI	5.23	**24.20**
12.5	4.21	**38.98**
12.5 + KI	3.63	**47.39**
25	2.99	**56.67**
25 + KI	2.23	**67.68**
50	1.85	**73.18**
50 + KI	1.30	**81.16**
75	1.59	**76.96**
75 + KI	1.14	**83.48**
100	1.48	**78.55**
100 + KI	0.61	**91.16**

Table 5. Values of the synergism parameter (S) for different concentrations of **LF-*Ch*** extract and 0.025% KI.

Conc. (mg / L)	**S**
12.5	0.88
25	1.02
50	1.08
75	1.06
100	1.84

From this table, it can be seen that the values of S for the **LF-*Ch*** extract and KI are greater than unity; except for the lower concentration. This result indicates that the increase in inhibitor efficiency is generated by the addition of KI to **LF-*Ch*** extract due to a synergistic effect and this may be related to adsorption of iodide ions on metal surfaces that caused the increase of adsorption of inhibitors. In addition, the synergistic effect is more pronounced for the optimal concentration.

2. 4. Immersion time

The impedance spectra of mild steel in 0,5 M H_2SO_4 + 5% EtOH with and without 100 mg/L of ***LF-Ch*** extract are shown in Figs 7a and 7b. The Nyquist plots were recorded after different immersion periods and each spectrum is characterized by a single full semi–circle.

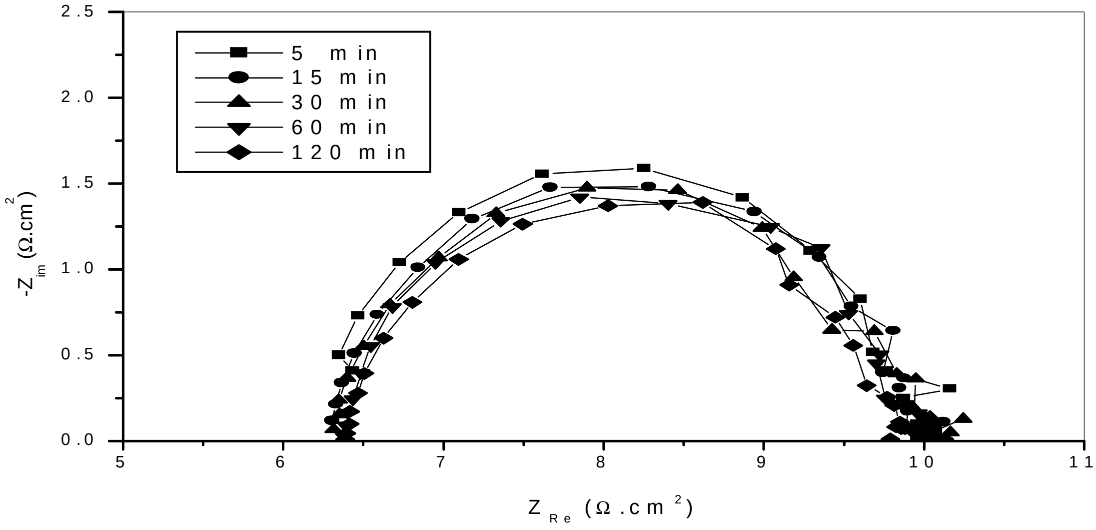

Figure 7a. Effect of immersion time on Nyquist plots of mild steel in 0.5M H_2SO_4 + 5% EtOH in absence of **LF-*Ch*** extract.

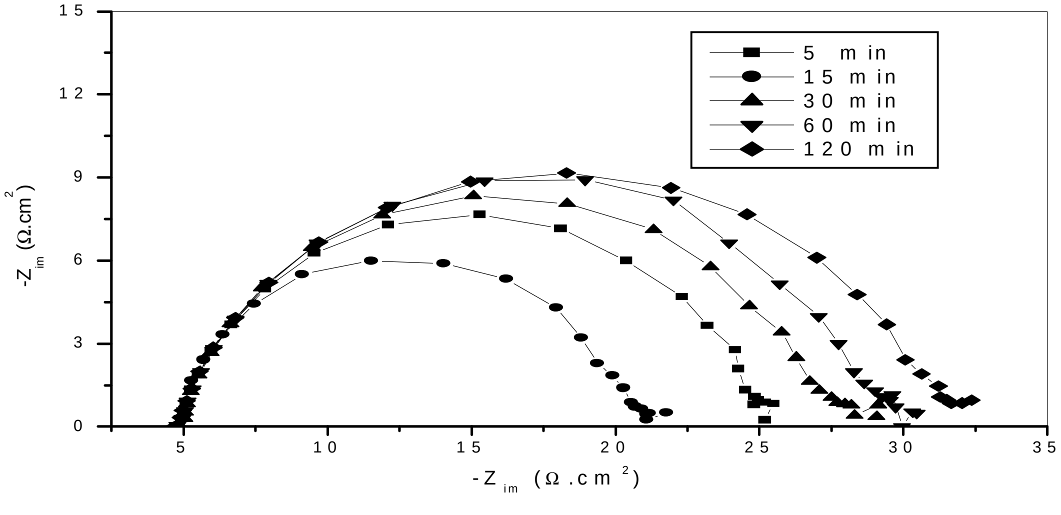

Figure 7b. Effect of immersion time on Nyquist plots of mild steel in 0.5M H_2SO_4 + 5% EtOH in presence of 100 mg/L of **LF-*Ch*** extract.

The calculated values of R_t and C_{dl} for mild steel immersed in the inhibited H_2SO_4 solution + 5% EtOH at different exposure times are shown in Table 6.

As can be seen from Table 6, we notice that as when the immersion time increases the difference between the double-layer capacity of mild steel immersed in acid alone and those in the presence of 100 mg/L of **LF-*Ch*** extract increases both in the absence and in the presence of 0.025% KI. This phenomenon is attributed to the film formed by the protective molecule inhibitors is thicker when the immersion time increases. In addition, we note that the inhibition efficiency increases from **81.81**% to **88.46%** after 2 hours of immersion.

As the thickness (d) of the protective film can be related to the film's capacitance (C) by the expression [8]:

$$d = \frac{\varepsilon_0 \varepsilon_r A}{C_{dl}} \tag{9}$$

where e_0, vacuum permeability; e_r, dielectric constant of the film ; A , area of electrode , it can be assumed that film thickness increases with decrease in C_{dl}

Table 6 . Effect of immersion time on R_t, C_{dl} and inhibition efficiency for mild steel in 0.5M H_2SO_4 + 5% EtOH with and without 100 mg/L of **LF-*Ch*** extract.

Immersion time (min)		**R_t (ohm cm^2)**	**C_{dl} (µF cm^{-2})**	**P (%)**
5	Blank	3.60	54.75	----
	100 mg/L	16.55	31.22	**78.24**
	100mg/L+0.025% KI	19.80	25.11	**81.81**
15	Blank	3.6	91.06	-----
	100 mg/L	20.60	24.60	**82.52**
	100mg/L+0.025% KI	24.41	26.33	**85.25**
30	Blank	3.56	146.15	-----
	100 mg/L	23.00	26.36	**84.52**
	100mg/L+0.025% KI	27.80	27.65	**87.19**
60	Blank	3.6	194.55	----
	100 mg/L	24.50	30.88	**85.30**
	100mg/L+0.025% KI	29.70	29.11	**87.88**
120	Blank	3.6	299.64	-----
	100mg/L	26.70	34.34	**86.51**
	100mg/L+0.025% KI	31.20	31.68	**88.46**

3.5. Adsorption

Basic information on the interaction between the inhibitor and the mild steel can be provided by the adsorption isotherm. The adsorption of the inhibitors can be described by two main types of interaction: physical adsorption and chemisorptions [32-36]. These are influenced by the chemical structure of the inhibitor, the type of the electrolyte and the charge and nature of the metal. The surface coverage θ of the metal surface by the adsorbed inhibitor was calculated assuming no change in mechanism of the cathodic reaction using the equation:

$$q = \frac{i_{0corr} - i_{icorr}}{i_{0corr}} \tag{10}$$

where I_{0corr} and I_{icorr} are the currents densities in the presence and absence of the inhibitor.

The θ values for different inhibitor concentrations at different temperatures were tested by fitting to various isotherms. By far the best fit was obtained with the Langmiur isotherm. According to this isotherm θ is related to concentration inhibitor C via:

$$\frac{C}{\theta} = \frac{1}{K} + C \tag{11}$$

where K is the adsorptive equilibrium constant of adsorption**.**

The plots of C/θ versus C yielded straight lines for **LF-*Ch*** extract and **LF-*Ch*** extract+ KI with slopes close to 1 (figure 8). This result indicates that the adsorption of compound under consideration on mild steel / acidic solution interface follows the Langmuir adsorption isotherm.

It should be noted that n the case of extract, inhibitory action is related to the intermolecular synergistic effect if the various components of natural oil or extract [37]. It is safely recommended to not determine ΔG_{ads} values since the mechanism of adsorption remains unknown.

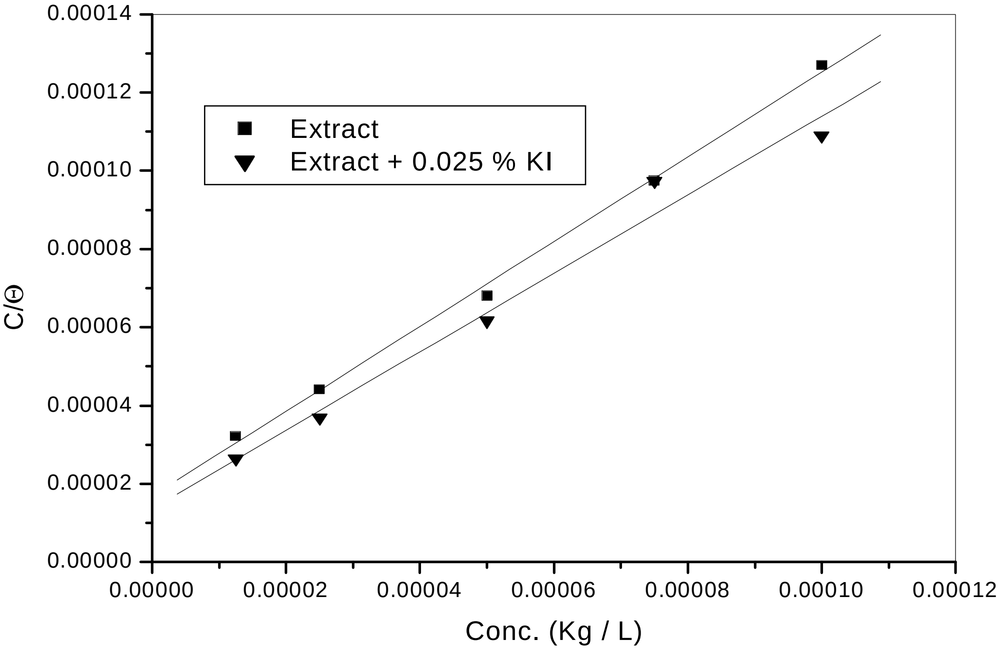

Figure 8. Langmuir adsorption isotherm of **LF-*Ch*** extract and **LF-*Ch*** extract+ KI on the mild steel surface

Conclusions

The main conclusions drawn from this study are:

- The data obtained from the Tafel polarization curves and electrochemical impedance spectroscopy (EIS), approve that **LF-*Ch*** extract is effective corrosion inhibitors for mils steel in 0.5 M sulfuric acid solution +5% EtOH.
- The inhibition efficiency improved with the increase of **LF-*Ch*** extract concentration, whether **LF-*Ch*** extract was used alone or in combination with KI. The increase in inhibitor efficiency is generated by the addition of KI to **LF-*Ch*** extract.
- The Tafel polarization curves indicate that both **LF-*Ch*** extract is mixed anodic-cathodic type inhibitors.
- The addition 0.025% KI to the solution lead to reduction in the essential usage of **LF-*Ch*** extract to achieve desirable inhibition efficiency.
- The values of the inhibition efficiency increased with the immersion time and leads to the formation of a protective film which grows with increasing exposure time.

References

1. Heydari M., Ravari F. B., Dadgarineghad A., *GU. J. Sci.* 24(3) (2011) 507.
2. Rozenfeld, I. L., “Corrosion Inhibitors”, *McGraw–Hill*, New York, (1981).
3. Benali O., Larabi L., Traisnel M., Gengembre L., Harek Y., *Appl. Surf. Sci.* 253 (2007) 6130.

4. Merah S., Larabi L., Benali O., Harek Y., *Pigm. Resin. Technol.* 37 (5) (2008) 291.
5. Benali O., Larabi L., Harek Y., *J. Appl. Electrochem.* 39 (2009) 769.
6. Benali O., Larabi L., Harek Y., *J. Saud. Chem. Soc.* 14 (2) (2010) 231.
7. Benali O., Larabi L., Tabti B., Harek Y., *Anti-Corros. Meth. Mat.* 52 (2005) 280.
8. Benali O., Larabi L., Mekelleche S.M., Harek Y., *J. Mater. Sci.* 41 (2006) 7064.
9. Eddy N. O.**,** *International J. Phys. Sci.* 4 (4) (2009) 165.
10. Bouyanzer A., Hammouti B., *Pigment and Resin Tech.* 33(5) (2004) 287.
11. Eddy N. O., Ekwumemgbo P., Odoemelam S. A., Int. J. Phys. Sci. 3(11) (2008) 275.
12. Eddy N. O., Odoemelam S. A., Akpanudoh N. W., *Res. J. Pure Appl. Sci.* 4(12) (2008) 1963.
13. Eddy N. O., Odoemelam S. A., Mbaba A. J., *Afri. J. Pure Appl. Chem.* 2(12) (2008) 132.
14. Selles C., Benali O., Tabti B., Larabi L., Harek Y., *J. Mater. Environ. Sci.* 3 (1) (2012) 206.
15. Ebenso E. E., Eddy N. O., Odiongenyi A. O., *Portug Electrochim. Acta.* 27(1) (2009) 13.
16. Bruneton, J., 2nd edition, Paris-South University, Lavoisier Publishing, France, (1993).
17. Benmehdi H., Hasnaoui O., Benali O., Salhi F., *J. Mater. Environ. Sci.* 3 (2) (2012) 320.
18. Scendo M., Uznanska J., *Internat. J. Corros.*, 2011, doi:10.1155/2011/761418
19. Shinde V., Sainkar S. R., Patil P. P., *Corros. Sci.*,47(6) (2005) 1352.
20. Özcan M., Gülfeza Kardaş R., Dehri İ, *Colloid Surf. A.* 325 (2008) 57.
21. Hukovic-Metikos M., Babic R., Grutac Z., *J. Appl. Electrochem.* 32 (2002) 35.
22. Mansfeld F., *Corrosion* 37 (1981) 301.
23. Mccafferty E., *Corros. Sci.* 39 (1997) 243.
24. Wu X., Ma H., Chen S., Xu Z., Sui A., *J. Electrochem. Soc.* 146 (1999) 1847.
25. Ma H., Chen S., Yin B., Zhao S., Liu X., *Corros. Sci.* 45 (2003) 867.
26. Gomma G. K., *Mater. Chem. Phy.* 55 (1998) 241.
27. Zhang D. Q., Gao L. X., Zhou G. D., *J. Appl. Electrochem.* 33 (2003) 361.
28. Ebenso E.E., Ibok U.J., Ekpe U.J., Umoren S., Jackson E., Abiola O.K., Oforka N.C., Martinez S., *Trans of SAEST* 39 (4) (2004) 117.
29. Oguzie E.E., *Mater. Chem. Phy.* 87 (2004) 212.
30. Okafor P. C., Osabor V. I., Ebenso E. E., *Pigm. Res. Tech.* 36 (5) (2007) 299.
31. Eduok U. M., Umoren S. A., Udoh A. P., Arab. J. Chem. 5 (3) (2012) 325.
32. Larabi L., Benali O., Harek Y., *Portug. Electrochim. Acta*, 24 (2006) 337.
33. Larabi L., Harek Y., Traisnel M., Mansri A., *J. Appl. Electrochem.*, 34 (2004) 833.
34. Benali O., Ouazene M., *Arab. J. Chem.* 4 (2011) 443.
35. Larabi L., Benali O., Harek Y., *Mater. Lett.*, 61 (2007) 3287.
36. Larabi L., Harek Y., Benali O., Ghalem S., *Prog. Org. Coat.* 54 (2005) 256.
37. Afia L., Salghi R., El Bazzi, Bazzi L., Errami M., Jbara O., Al-Deyab S.S., Hammouti B., *Int. J. Electrochem. Sci.* 6 (2011) 5918.